

TECHNICAL REVIEW

No. 3 — 1982

Contents

Sound Intensity (Part I. Theory) by S. Gade.....	3
--	---

SOUND INTENSITY (Part I Theory)

by

S. Gade, M.Sc.

ABSTRACT

In this article the theoretical concept of sound intensity (a quantity describing the net flow of acoustic energy) is described, and shows how it makes a distinction between the active and reactive parts of sound fields. Furthermore, it is shown how sound intensity can be measured over a wide frequency range by the use of a specially designed probe, consisting of a pair of closely spaced pressure microphones.

The different principles of signal processing are discussed, such as the digital filtering employed in the Brüel & Kjær Sound Intensity Analyzing System Type 3360, and the use of the Fast Fourier Transform (FFT) technique. The digital filter sound analyzing system operates in real time and calculates third octave spectra more than 100 times faster than an analyzer based upon FFT-technique.

The high and low frequency limitations as well as the near field limitations with the two microphone technique are outlined and shown how they are minimised. Calibration procedure is also described.

In Part II of the article (Technical Review No.4 – 1982) the practical aspects of instrumentation will be discussed and applications illustrated.

SOMMAIRE

Cet article décrit le concept théorique de l'intensité acoustique (une quantité décrivant le flux d'énergie acoustique moyen), et montre la distinction qui est faite entre les parties active et réactive des champs sonores. De plus, il y est montré comment l'intensité acoustique peut être mesurée sur une large gamme de fréquence en utilisant une sonde spécialement conçue, comprenant une paire de microphones de pression rapprochés.

Les différents principes de traitement du signal sont examinés, comme par exemple le filtrage numérique utilisé sur le Système d'analyse d'intensité acoustique Brüel & Kjær Type 3360 et la technique utilisant la transformée de Fourier rapide (FFT). Les filtres numériques des systèmes d'analyse sonore fonctionnent

en temps réel et calculent des spectres de 1/3 d'octave 100 fois plus vite qu'un analyseur basé sur des techniques FFT.

Les limites de haute et basse fréquence, et les limites de champ rapproché avec la technique des deux microphones sont mises en valeurs, ainsi que la façon dont elles sont minimisées. La procédure d'étalonnage est également décrite.

Dans la seconde partie de cet article (Revue technique No.4-1982) les aspects pratiques des appareils seront décrits avec des illustrations d'applications..

ZUSAMMENFASSUNG

In diesem Artikel wird das theoretische Konzept der Schallintensität (einer Größe, die den Nettofluß der Schallenergie beschreibt) beschrieben, und gezeigt, wie sich aktive und reaktive Schallfeldteile unterscheiden lassen. Außerdem wird gezeigt, wie man mit Hilfe einer speziell konstruierten Sonde, bestehend aus zwei dicht beieinander platzierten Druck-Mikrofonen, die Schallintensität über einen weiten Frequenzbereich messen kann.

Es werden verschiedene Prinzipien der Signalverarbeitung diskutiert u.a. digitale Filter, wie sie im Brüel & Kjær-Schallintensitätsanalysator 3360 verwendet werden, und FFT-Technik. Der Schallintensitätsanalysator arbeitet in Echtzeit und berechnet Terzspektren mehr als 100mal so schnell, wie es nach der FFT-Technik möglich ist.

Begrenzungen der Zwei-Mikrofontechnik bei hohen und tiefen Frequenzen sowie im Nahfeld werden ebenfalls diskutiert und gezeigt, wie sich diese minimieren lassen. Daneben wird die Kalibrierung beschrieben.

Im zweiten Teil des Artikels (Technical Review Nr. 4 — 1982) werden praktische Anwendungen der Geräte diskutiert.

Introduction

In the last decade there has been an increasing interest in measuring the acoustic quantity, sound intensity, mostly for the investigation and localization of noise sources.

Furthermore, with the aid of an intensity meter, it is possible to measure the sound power emitted by machinery even in the presence of high background noise.

The theoretical background for intensity measurements was already described by H.F. Olson as early as in 1932. Unfortunately, the problems involved in adjusting and calibrating intensity meters have pre-

vented the development of such instruments based upon conventional techniques.

The advent of real-time analysis using digital filtering techniques for signal processing has been the major breakthrough for the precision with which acoustic intensity measurements can be carried out.

1. Sound Intensity

Sound Intensity or Energy Flux is a *vector* quantity which describes the amount and the direction of net flow of acoustic energy at a given position. Hence the dimension is Energy per Time per Area and the unit is (W/m²).

This is in contrast to sound pressure which is a *scalar* quantity (magnitude only).

It can be shown (see appendix A) that in a medium without mean flow, the intensity vector equals the time averaged product of the instantaneous pressure and the corresponding instantaneous particle velocity at the same position.

$$\vec{I} = \overline{p(t) \cdot \vec{u}(t)} \quad (1.1)$$

(where the bar indicates time averaging) or in direction, r as

$$I_r = \overline{p(t) \cdot u_r(t)} \quad (1.2)$$

This equation has the well known electrical analogy, power = voltage \times current.

If the sound field is sinusoidal, use of complex notation is convenient. In terms of complex pressure and complex particle velocity the intensity vector is given by

$$\vec{I} = 1/2 \operatorname{Re} (p \cdot \vec{u}^*) \quad (1.3)$$

or in direction, r as

$$I_r = 1/2 \operatorname{Re} (p \cdot u_r^*) \quad (1.4)$$

where time averaging is implicitly given in the formula by the factor $1/2$ and where u^* indicates the complex conjugate of u .

2. Active and Reactive Sound Fields

One of the properties of Sound Intensity is the distinction it makes between the active and the reactive part of sound fields, a property

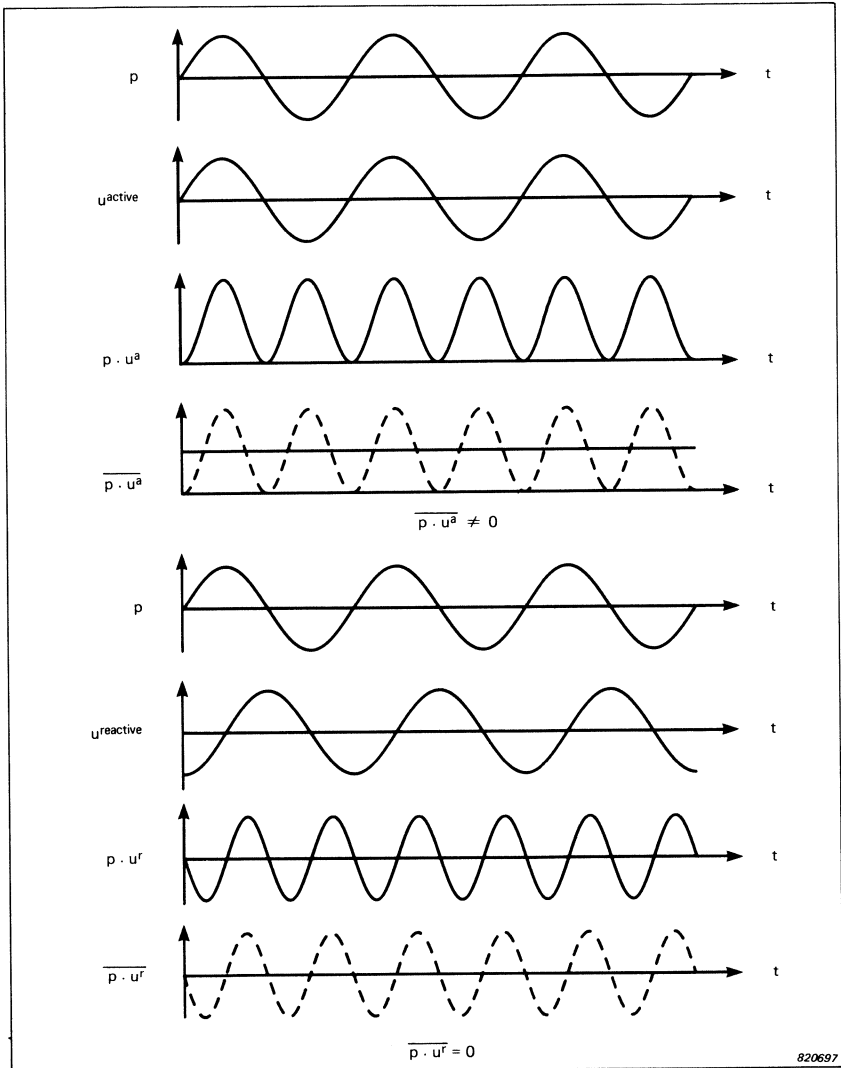


Fig. 1. The active and reactive part of sound fields

sound pressure does not have. An intensity meter responds only to the active part and ignores the reactive part of sound fields.

The particle velocity, u can actually be split up into two components, u^{active} and u^{reactive} , where u^{active} is in phase with the pressure p and u^{reactive} is 90° out of phase with the pressure p . Only the in-phase particle velocity component, u^{active} will give a time averaged product with pressure which is unequal to zero, as shown in Fig.1.

A plane wave propagating in free field is an example of a purely active sound field. In fact in this case the particle velocity can be calculated from the pressure by use of the acoustical analogy of Ohm's law (current = voltage/resistance):

$$u = p/\rho c \quad (2.1)$$

The magnitude of the intensity is thus given by

$$|\vec{I}| = \overline{p \cdot u} = \overline{p^2/\rho c} = \rho_{\text{rms}}^2/\rho c \quad (2.2)$$

where ρc is the impedance of the medium. In fact, when free-field condition is given, the intensity can be determined indirectly from the sound pressure.

In reactive sound fields the intensity is zero, which means that in this case there is no net flow of energy. One example is an ideal standing

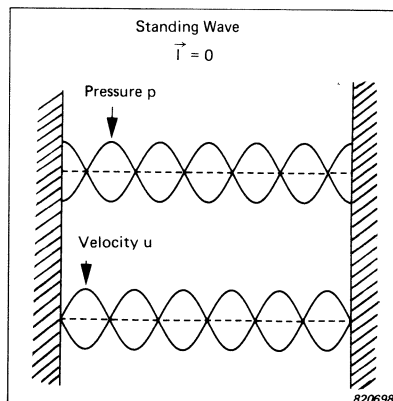


Fig. 2. Standing wave

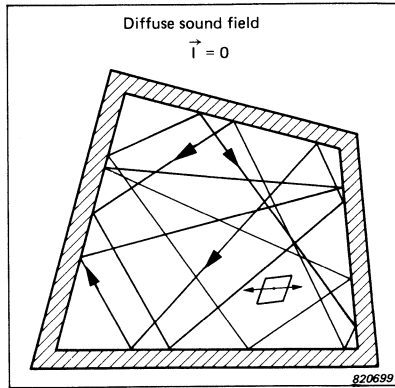


Fig. 3. Diffuse sound field

wave, since the particle velocity u is 90° out of phase with the pressure p . The pressure has its maximum values at the walls where the particle velocity is zero (see Fig.2), corresponding to a 90° phase shift between the two quantities.

Another example of a purely reactive sound field is an ideal diffuse sound field, where—by definition—the energy flow at a given position is the same in all directions. Hence, there is no *net* flow of acoustic energy at any points—the sound intensity is zero (see Fig.3).

However, in a diffuse sound field the intensity of sound energy passing through a plane of unit area from one side only is:

$$I = \frac{p_{rms}^2}{4\rho c} \quad (2.3)$$

3. How can Sound Intensity be Measured

To measure sound intensity, the instantaneous pressure and the corresponding particle velocity must be known. The pressure can easily be measured and in fact sound pressure is the most commonly measured quantity in acoustics.

However, a direct measurement of particle velocity is very difficult, requiring the use of devices like hot wire anemometers, or delicately suspended mica discs.

A different method using 2 identical pressure microphones is preferable, since this method allows an easy calibration of the system.

The method is based upon Newton's second law, that is the Equation of Motion (mass \times acceleration = force),

$$\rho \cdot \frac{\partial \vec{u}}{\partial t} = - \text{grad } p \quad (3.1)$$

also called Euler's Relation, where ρ is the density of air.

In one direction, r we have

$$\rho \cdot \frac{\partial u_r}{\partial t} = - \frac{\partial p}{\partial r} \quad (3.2)$$

Since the pressure gradient is proportional to the particle acceleration, the particle velocity can be obtained by integrating the pressure gradient with respect to time, see Appendix B.

$$u_r = - \frac{1}{\rho} \int \frac{\partial p}{\partial r} dt \quad (3.3)$$

In practice, the pressure gradient can be approximated by measuring the pressures, p_A and p_B , at two closely spaced points, A and B, and dividing the pressure difference $p_B - p_A$ by the transducer separation distance Δr , thus giving the following estimate for the particle velocity component \hat{u}_r in the direction r :

$$\hat{u}_r = - \frac{1}{\rho \Delta r} \int (p_B - p_A) dt \quad (3.4)$$

This approximation is valid as long as the separation is small compared with the wavelength ($\Delta r \ll \lambda$).

A practical sound intensity probe can therefore consist of two closely spaced pressure microphones, allowing for measurement of both pressure and the component of the pressure gradient along a line joining the centres of the microphones. Hence, the magnitude and the direction of the component of the intensity vector along this line is measured as shown in Fig.4.

Note, that it is the phase gradient of the pressure which gives a non-zero real intensity vector (see Appendix C).

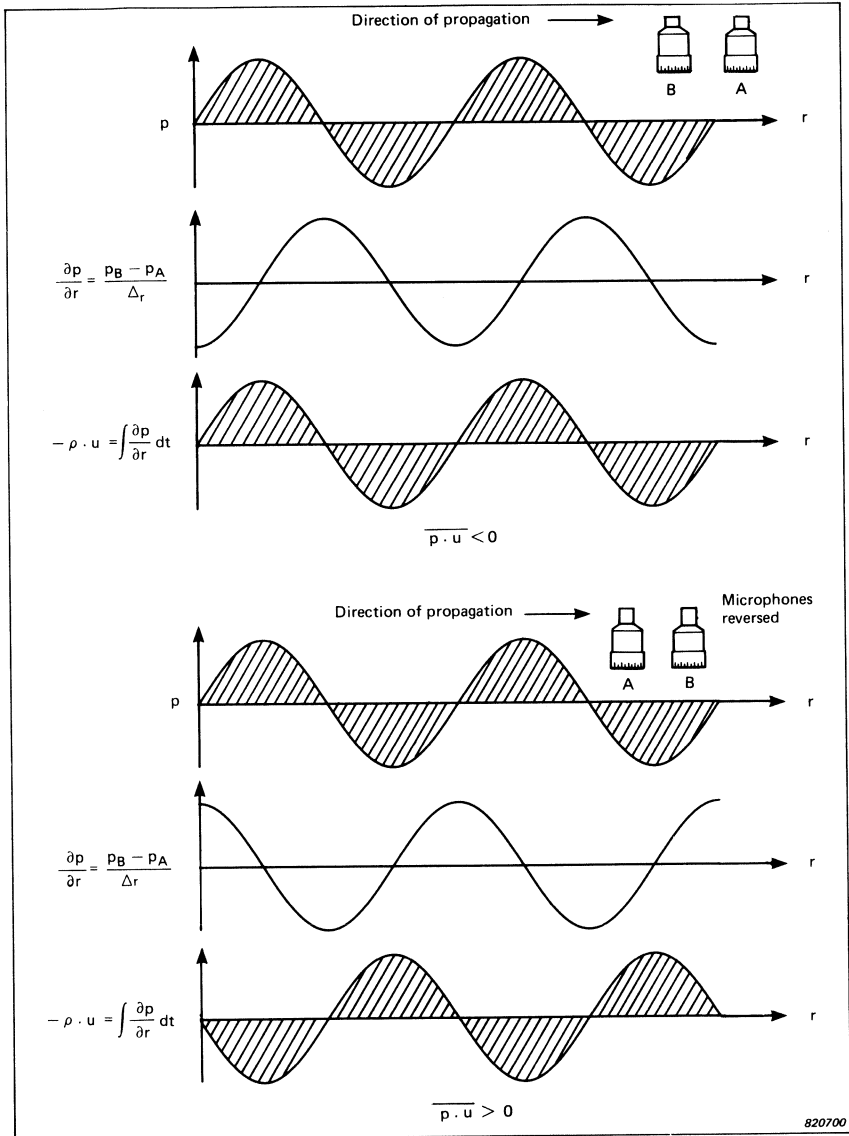


Fig. 4. Example of intensity calculation for a plane wave propagating in the r -direction.
 Note how the sign is directly given by the orientation of the probe (for time integration, see Appendix B)

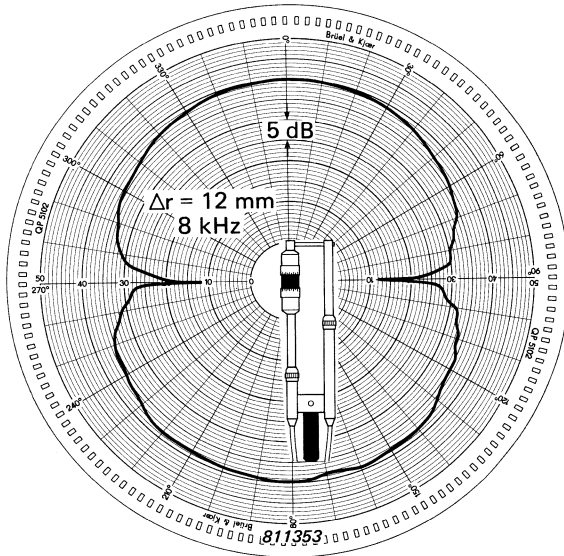
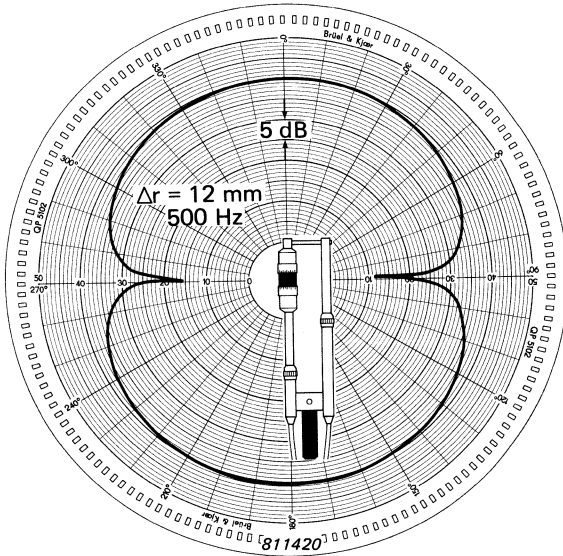


Fig. 5. Directional characteristics at 500 Hz and 8 kHz for the probe Type 3519 fitted with 1/2" microphones and 12 mm spacer

As already mentioned, it is an intensity vector *component* not the intensity vector, that is measured by this technique.

The consequence is that the theoretical directional characteristics of the microphone probe is a cosine function

$$|I_r| = |\vec{I}| \cdot \cos \alpha \quad (3.5)$$

where α is the angle between the direction of net energy flow and the orientation of the probe.

Fig.5 shows the practical directional characteristics of the B & K intensity probe showing broad maxima and very narrow minima.

4. Signal Processing

For processing the signals from the transducers two main lines of approach are in current use today. One approach is a direct method which can be implemented by analogue as well as digital techniques. The second approach, the indirect method can only be implemented by use of digital technique.

4.1. Direct Method

The sound intensity vector component in the direction r is calculated from:

$$\hat{I}_r = \overline{p \cdot u_r} = -\frac{1}{2\rho \Delta r} \overline{(p_A + p_B) \int (p_B - p_A) dt} \quad (4.1)$$

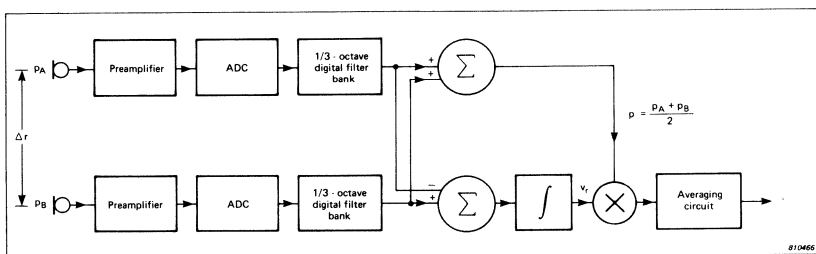


Fig. 6. The two-microphone technique and the direct method employed by the 3360 system to measure sound intensity

where the sound pressure is taken as being the mean pressure $(p_A + p_B)/2$ between the two microphones, and where the velocity is calculated from equation 3.4.

Fig.6 shows a block diagram of a practical real-time sound intensity meter, including $1/3$ octave digital filters. Notice how the block diagram follows the equation step by step.

B & K Sound Intensity Analyzing System Type 3360 is based upon this principle with an analysis range from 3,2 Hz to 10 kHz third octave band centre frequencies.

4.2. Indirect Method

A Dual Channel FFT (Fast Fourier Transform) analyzer can be used for intensity calculations within the FFT-limitations (blockwise analysis). It is shown in Appendix D that the intensity can be calculated from the imaginary part of the cross-spectrum between the 2 microphone signals.

$$\hat{I}_r = - \frac{1}{\omega \rho \Delta r} \text{Im } G_{AB} \quad (4.2)$$

Today, this forms a commonly used method of calculating sound intensity. However, a computer or a calculator is required to carry out the final calculations. Unfortunately this method has certain disadvantages. One of these is that sound measurements are normally specified in octaves and third octaves, and the calculation of these from narrow band spectra is a time-consuming procedure, usually requiring multi-pass analysis and synthesis, which cannot be performed in real time (Ref.[11]).

5. Calibration

One of the advantages of using the 2 pressure microphone technique is the ease with which very accurate calibration can be carried out, using a pistonphone (B & K Type 4220), which provides a 124 dB re. 20 μ Pa sound pressure level at 250 Hz.

The reference pressure p_o for sound pressure levels is 20 μ Pa and the reference intensity I_o for intensity levels is 1 pW/m^2 . These reference values have been chosen so that for a freely propagating plane wave 0 dB sound pressure level corresponds to 0 dB sound intensity level as shown in equations 5.1 and 5.2.

$$I = \frac{p_{rms}^2}{\rho c} \quad (5.1)$$

for $p = 20 \mu Pa$ we have

$$I_o \approx \frac{(20 \cdot 10^{-6})^2}{400} W/m^2 = 1 \rho W/m^2 \quad (5.2)$$

since $\rho c \approx 400 \text{ kg/m}^2 \text{ s}$.

A calibrated barometer is provided with the pistonphone to determine the necessary correction for the ambient atmospheric pressure, since the sound pressure of the pistonphone is proportional to the ambient pressure

$$\Delta L_p (p_{amb}) = + 10 \log_{10} (p_{amb}/p_o)^2 = + 20 \log_{10} (p_{amb}/p_o) \quad (5.3)$$

where $p_o = 1 \text{ atm}$.

The air density is also proportional to the ambient pressure, so from equation 4.1 it follows that the correction term due to ambient pressure for intensity calibration by use of a pistonphone is

$$\begin{aligned} \Delta L_I (p_{amb}) &= + 20 \log_{10} (p_{amb}/p_o) - 10 \log_{10} (p_{amb}/p_o) \\ &= + 10 \log_{10} (p_{amb}/p_o) \end{aligned} \quad (5.4)$$

Therefore when calibrating the system for use in sound intensity mode only half the atmospheric pressure correction indicated on the barometer scale must be applied to each microphone.

Besides the air density is inversely proportional to the absolute temperature T , which leads to the temperature correction term

$$\Delta L_I (temp) = + 10 \log_{10} (T/T_o) \quad (5.5)$$

where $T_o = 293^\circ K (20^\circ C)$

In general, these correction terms can often be ignored since they are relatively small. For a temperature of $40^\circ C$ and an ambient pressure of 750 mbar (Mexico City, 2300 meters above sea level) the correction term is only 1,0 dB.

6. High Frequency Limitations

The use of the 2 microphone technique imposes limitations on the useful frequency range of the measuring system. A principal systematic error is inherent in the approximation of the pressure gradient by a finite pressure difference. This error is most severe at high frequencies. The approximation error can be calculated for ideal sound fields and ideal sound sources. Since the sound field is seldom known in sufficient detail, such calculations only give an idea of the useful frequency range.

For a plane sinusoidal wave, which for simplicity is assumed to propagate along the axis joining the microphones, the estimate of the approximated value \hat{I}_r is related to the actual intensity I_r by the expression (Appendix E)

$$\frac{\hat{I}_r}{I_r} = \frac{\sin(k \Delta r)}{(k \Delta r)} \quad (6.1)$$

where Δr is the distance between the microphones
and k is the wave number

Apparently the intensity is underestimated, particularly at high frequencies and for large microphone separation distances.

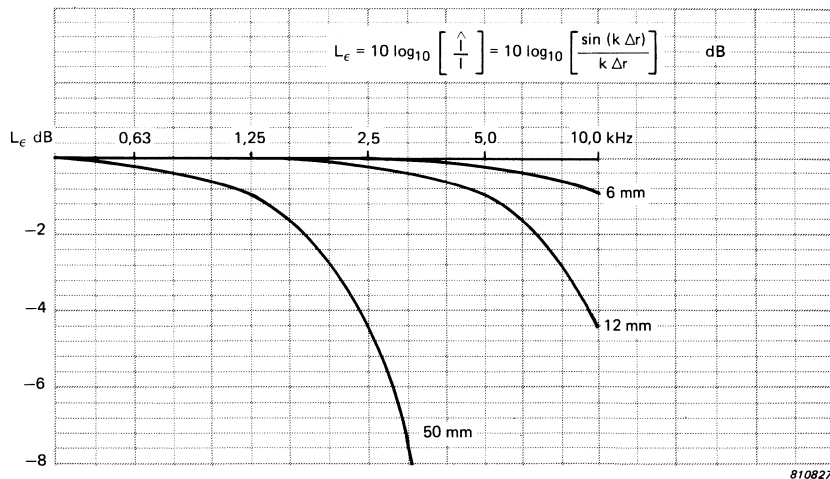


Fig. 7. Approximation error, L_ϵ , at high frequencies for various spacers

Fig.7 shows the approximation error in dB, denoted by L_ϵ at high frequencies for various separation distances (choice of spacer) between the two microphones.

7. Nearfield Limitations

Another bias error occurs, if the intensity changes along the probe, i.e. if the intensity is different at the two microphone positions.

For a spherical wave, from a monopole source, it can be shown (Appendix F) that the error between the approximated sound intensity and the exact intensity is given by

$$\frac{\hat{I}_r}{I_r} = \left(\frac{\sin k \Delta r}{k \Delta r} \right) \cdot \left(\frac{r^2}{r_1 \cdot r_2} \right) = \left(\frac{\sin k \Delta r}{k \Delta r} \right) \cdot \left(1 - 1/4 \left(\frac{\Delta r}{r} \right)^2 \right)^{-1} \quad (7.1)$$

where the distances Δr , r , r_1 and r_2 are shown in Fig.8.

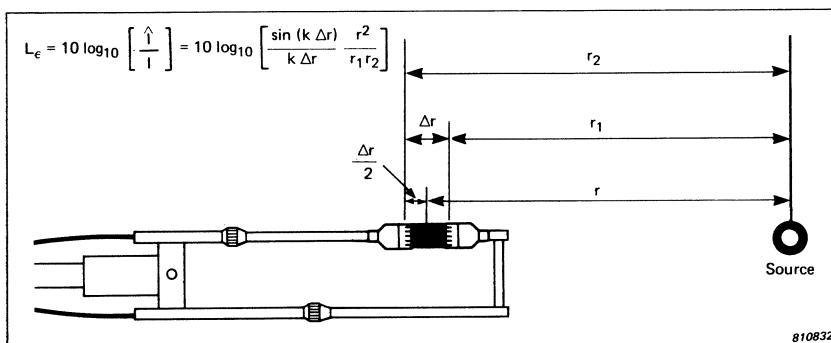


Fig. 8. Definition of the quantities used in the expression for L_ϵ

The approximation error is not only a function of $k \Delta r$ but also of $\Delta r/r$. Fig.9 shows this function, and it is seen that if $r > 2 \cdot \Delta r$ this error is negligible, while for $r = \Delta r$ the error is an overestimation of approximately 1 dB.

For dipole sources it can be shown (Ref.[1], [2]) that the error formula due to the finite microphone separation is

$$\frac{\hat{I}_r}{I_r} = \left(\frac{\sin k \Delta r}{k \Delta r} \right) \cdot \left(\frac{r^2}{r_1 \cdot r_2} \right) \cdot \left(1 + \frac{1 - k \Delta r \cdot \cot(k \Delta r)}{k^2 r_1 r_2} \right) \quad (7.2)$$

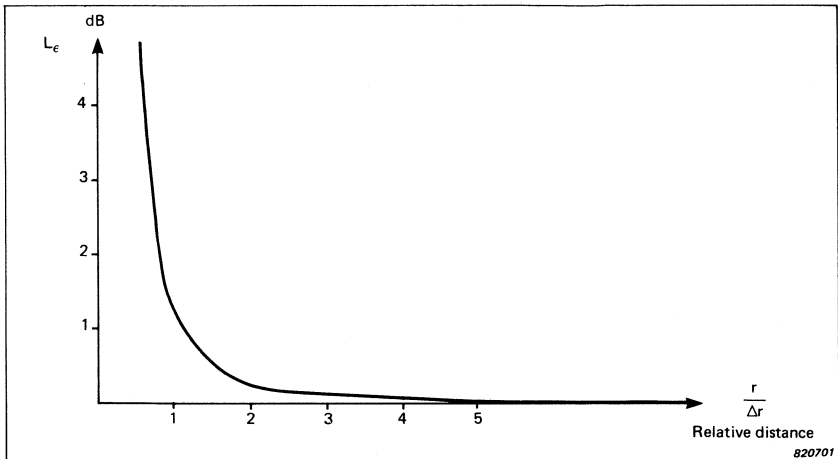


Fig. 9. Proximity approximation error for a monopole source

A similar formula for quadruple sources is given in Ref.[1], [2].

From these functions it can be shown, that if the distance between the probe and the acoustic centre of the different types of sources is greater than 2 to 3 times the microphone spacing a proximity error of less than 1 dB is achieved (see Table 1).

Source Type	Proximity error less than 1 dB for r
Monopole	$> 1,1 \Delta r$
Dipole	$> 1,6 \Delta r$
Quadrupole	$> 2,3 \Delta r$

820045

Table 1. Proximity approximation error for various ideal sound sources

This indicates that intensity measurements can be performed in the near field of even rather complex sound sources without introducing significant errors.

Note that for most situations, the acoustic centre of a noise source is situated behind the surface of the source. This means that the acoustic

distance between the probe and the source, normally is much larger than the physical distance. Since the position of the acoustic centre of complex noise sources are seldom known, any attempt to correct the measured intensity values by means of eqn. 7.1, 7.2 would not be advisable.

8. Low Frequency Limitations

The calculation of particle velocity by use of the 2 microphone technique is based upon measurement of the phase gradient rather than the modulus of pressure gradient of the sound field. This is indicated in Appendix C.

The quantity $k \cdot \Delta r$ is in fact the phase difference between the two microphone positions in a plane sinusoidal wave where the probe is oriented in the direction of propagation.

If a phase mismatch φ exists between the two measuring channels, the detected phase difference will become $k \Delta r \pm \varphi$ instead of $k \Delta r$ leading to the modified approximation formula

$$\frac{\hat{i}}{I} = \frac{\sin(k \Delta r \pm \varphi)}{k \Delta r} \tag{8.1}$$

Evidently a possible phase mismatch is most critical for *small* values of microphone spacings, and at *low* frequencies. This sets the lower frequency limit for practical systems.

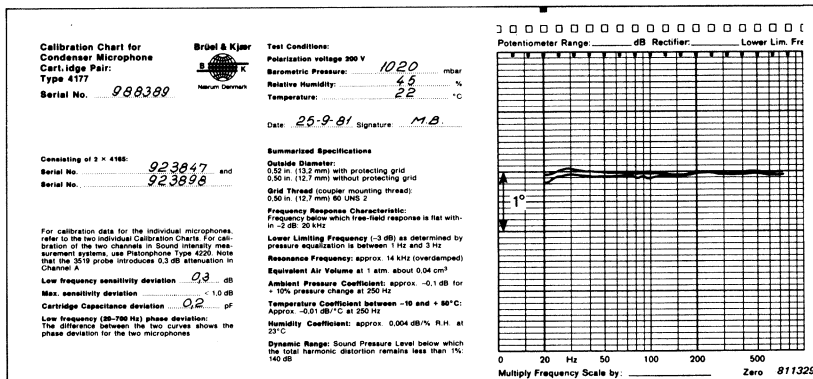


Fig. 10. Typical calibration chart for Condenser Microphone Cartridge pair 4177

Thus the two microphones used in the probe system should be selected by matching their phase responses to minimize this error. Typical phase matching of the B & K Sound Intensity Probe Type 3519 is shown in Fig.10.

The digital approach of the B & K Sound Intensity Analyzer Type 2134 ensures phase matching of the 2 measuring channels better than $0,3^\circ$ for the total system.

The maximum approximation error at low frequencies for various spacers for a phase matching of $0,3^\circ$ is shown in Fig.11. The curves indicate that the error takes form of an underestimation and is less than 1 dB at 30 Hz for a 50 mm spacer. If the microphones are interchanged the error takes form of an overestimation of the intensity (See Fig.12). For very low frequency measurements larger microphone separation is required to minimize the error.

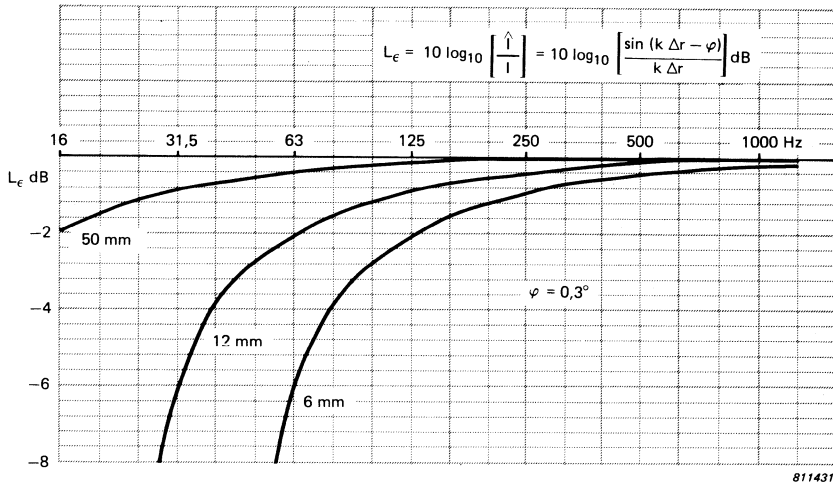


Fig. 11. Maximum approximation error, L_ϵ , at low frequencies for various spacers for a phase matching of $0,3^\circ$

Frequency Ranges for the various microphone and spacer configurations for the Sound Intensity Probe Type 3519 are shown in Fig.15.

Phase mismatch actually results in distortion of the directional characteristics of the probe. The direction for minimum sensitivity is deflected

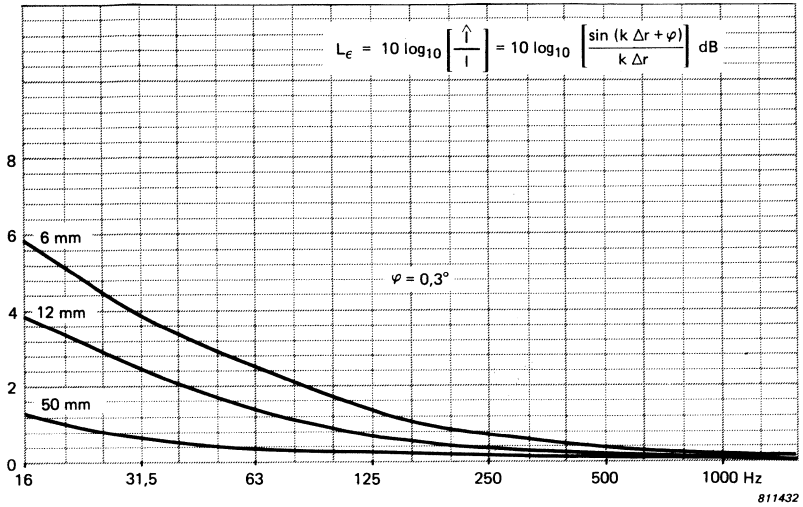


Fig. 12. Overestimation of the intensity

by an angle ψ from the plane perpendicular to the probe as shown in Fig.13. Geometrical considerations lead to

$$\psi = \arcsin \frac{\varphi}{k \Delta r} \quad (8.2)$$

The graphs in Fig.14 show the directional offset angle as a function of

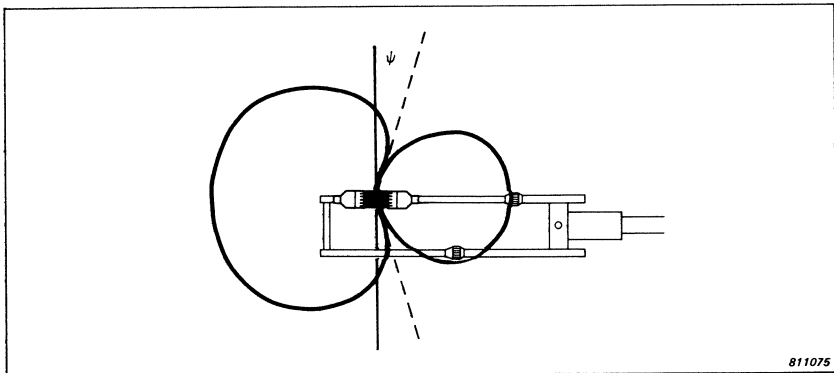


Fig. 13. Angular displacement of the minima axes

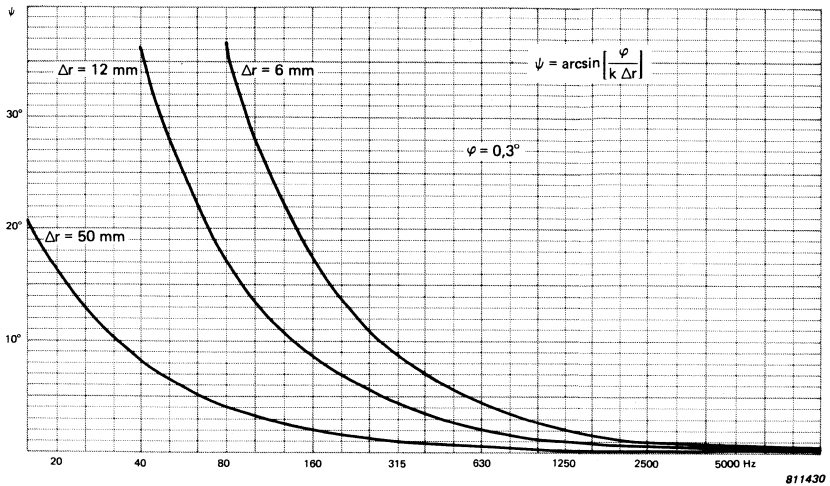


Fig. 14. Angular displacement of the minima axes as a function of Δr for $\varphi = 0,3^\circ$

frequency for a phase matching of $0,3^\circ$ and various microphone separation distances.

Note, that for the frequency limits shown in Fig.15 the offset angle for the B & K probe will be less than 10° – typically better.

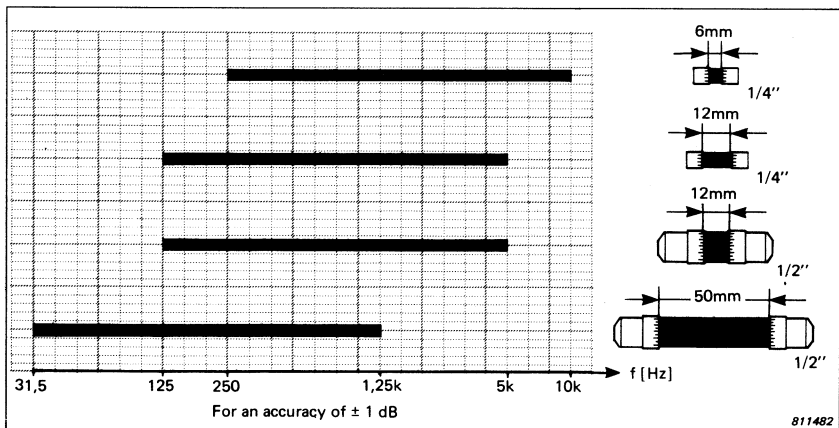


Fig. 15. Frequency Range for the various microphone and spacer configuration for a measurement accuracy of ± 1 dB

References

- [1] THOMPSON, J.K. & TREE, D.R.: "Finite difference approximation errors in acoustic intensity measurements." *Journal of Sound and Vibration*, 1981 75(2), pp.229-238. And discussion by Ref.[2].
- [2] ELLIOT, S.J.: "Errors in Acoustic Intensity Measurements." *Journal of Sound and Vibration*, 1981 78(3), pp.439-445.
- [3] JACOBSEN, F.: "Measurement of sound intensity." Report 28, 1980, *Acoustics Laboratory of the Danish Technical University*.
- [4] CHUNG, J.Y. & POPE, J.: "Practical Measurement of acoustic intensity – the two-microphone cross-spectral method." *Proc. Inter-Noise 78*, pp.893–900.
- [5] CHUNG, J.Y.: "Cross-spectral method of measuring acoustic intensity without error caused by instrument phase mismatch." *J. Acoust. Soc. Am.* 64, 1978, pp.1613–1616.
- [6] ROTH, O.: "A Sound Intensity Real-Time Analyzer." *Acoustic Intensity - Senlis 1981*, pp.69–74.
- [7] RASMUSSEN, G. & BROCK, M.: "Acoustic Intensity Measurement Probe." *Acoustic Intensity – Senlis 1981*, pp.81-84.
- [8] FRIUNDI, F.: "The utilization of the Intensity-Meter for the investigation of sound radiation of surfaces." *Unikeller* 1977.
- [9] LAMBERT, J.M.: "The application of a Modern Intensity-Meter to Industrial Problems: Example of in-situ sound power determination." *Internoise 79*, pp. 227-231.

- [10] BRÜEL & KJÆR: "Sound Intensity Analysing System Type 3360." *Product Data*.
- [11] RANDALL, R.B. & UPTON, R.: "Digital Filters and FFT Technique." *B & K Technical Review*, No.1-1978.
- [12] BENDAT, J.S. & PIERSOL, A.G.: "Engineering Applications of Correlation and Spectral Analysis." *Wiley Interscience*, 1980.
- [13] CHUNG, J.Y. & BLASER, D.A.: "Transfer function method of measuring acoustic intensity in a duct system with flow." *J. Acoustic. Soc. Am.* 68(6), Dec. 1980, pp. 1570-1577.

APPENDIX A

Sound Intensity

The intensity I_r is defined as

$$I_{r,inst} = \frac{dE_r}{dt \cdot dA} \quad (\text{A.1})$$

where dE_r is the energy passing through the area dA perpendicular to the direction of propagation in the period of time dt , see Fig.A1.

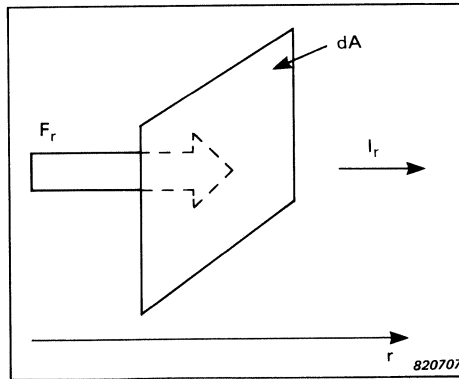


Fig. A1. Energy transport through the area dA in the direction r due to the total force F_r acting on the surface in the direction r

The energy transport dE_r is equal to the amount of work done upon the area dA in the direction r due to the total force F_r , i.e.

$$dE_r = F_r \cdot dr = p_t \cdot dA \cdot dr \quad (\text{A.2})$$

where $p_t = p_a + p$ is the total pressure consisting of two parts p_a , the ambient (static) pressure and p , the sound pressure.

Hence the instantaneous intensity is

$$I_{r,inst} = p_t \cdot \frac{dr}{dt} = p_a \cdot u_r + p \cdot u_r \quad (\text{A.3})$$

where $\frac{dr}{dt} = u_r$ is the particle velocity in the direction r .

The term containing the ambient pressure p_a , which is a pressure dc-component, will be averaged to zero, when time averaging is performed. Therefore, the intensity vector component in the direction r is equal to the time-averaged product of the instantaneous sound pressure and the corresponding instantaneous particle velocity in the direction r . The bar indicates time averaging.

$$I_r = \overline{p \cdot u_r} \quad (\text{A.4})$$

This is of course only true when the particle velocity does not contain a dc-component, that is when the medium is without mean flow. In Ref.[13] it is shown that even for mean-flow mach numbers below 0,1 in a duct considerable error in the intensity calculation might be induced by neglecting the effect of flow, that is the term $p_a \cdot u_{mean}$.

However, other researchers have reported good results in free air by use of a windscreen.

For the intensity probe, a zeppelin shaped windscreen made of open cell polyurethane seems to give the best performance (Ref.[7]).

In three dimensions the intensity vector can be written as

$$\begin{aligned} \vec{I} &= \overline{p \cdot u_x + p \cdot u_y + p \cdot u_z} \\ &= \overline{p \cdot \vec{u}} \end{aligned} \quad (\text{A.5})$$

If the sound field is sinusoidal we have:

$$\begin{aligned} p &= p_o \cdot \cos(\omega t + \phi_1) \\ \vec{u} &= \vec{u}_o \cdot \cos(\omega t + \phi_2) \end{aligned} \quad (\text{A.6})$$

Now

$$\begin{aligned}\vec{I} &= \overline{p \cdot \vec{u}} = \frac{1}{T} \int_0^T p_o \cdot \vec{u}_o \cdot \cos(\omega t + \phi_1) \cdot \cos(\omega t + \phi_2) dt \\ &= \frac{1}{T} \int_0^T p_o \cdot \vec{u}_o \cdot \frac{1}{2} [\cos(2\omega t + \phi_1 + \phi_2) + \cos(\phi_1 - \phi_2)] dt\end{aligned}$$

For sufficiently large T

$$\begin{aligned}\vec{I} &= \frac{1}{2} p_o \cdot \vec{u}_o \cdot \cos(\phi_1 - \phi_2) \\ &= p_{rms} \cdot \vec{u}_{rms} \cdot \cos(\phi_1 - \phi_2)\end{aligned}\tag{A.7}$$

The intensity not only depends on the magnitude of the pressure and particle velocity, but also on the cosine of the phase difference between the two quantities.

For sinusoidal sound fields complex notation is often convenient.

A complex number, A , consists of a real part and imaginary part and can be written as follows:

$$A = A_o \cdot e^{jx} = A_o \cdot [\cos x + j \sin x]\tag{A.8}$$

where
$$j = \sqrt{-1} \text{ or } j^2 = -1$$

The complex conjugate of A , also denoted as A^* , is defined as

$$A^* = A_o \cdot e^{-jx} = A_o \cdot [\cos x - j \sin x]\tag{A.9}$$

that is a change of the sign of the imaginary part.

Using complex notation, p and \vec{u} can be written as

$$\begin{aligned}p &= \text{Re} [p_o \cdot e^{j(\omega t + \phi_1)}] \\ \vec{u} &= \text{Re} [\vec{u}_o \cdot e^{j(\omega t + \phi_2)}]\end{aligned}\tag{A.10}$$

Equations A.6 and A.10 are identical.

And by complex notation, the intensity can be calculated from

$$\begin{aligned}\vec{I} &= \text{Re} \left[\overline{\rho \cdot \vec{u}^*} \right] \\ &= \text{Re} \left[\frac{1}{2} \cdot \rho \cdot \vec{u}^* \right]\end{aligned}\tag{A.11}$$

since

$$\begin{aligned}\text{Re} \left[\frac{1}{2} \rho \cdot \vec{u}^* \right] &= \text{Re} \left[\frac{1}{2} \rho_o \cdot \vec{u}_o \cdot e^{j(\omega t + \phi_1)} \cdot e^{-j(\omega t + \phi_2)} \right] \\ &= \text{Re} \left[\frac{1}{2} \rho_o \cdot u_o \cdot e^{j(\phi_1 - \phi_2)} \right] \\ &= \frac{1}{2} \rho_o \cdot \vec{u}_o \cdot \cos(\phi_1 - \phi_2)\end{aligned}\tag{A.12}$$

Equations A.7 and A.12 are identical.

APPENDIX B

Time Integration

For sinusoidal sound fields and ideal time integration we have

$$p(x,t) = p_0 \cdot e^{j(\omega t - kx)} \quad (\text{B.1})$$

$$\begin{aligned} \int p(x,t) dt &= p_0 \cdot e^{-jkx} \int e^{j\omega t} dt \\ &= p_0 \cdot e^{-jkx} \frac{1}{j\omega} \cdot e^{j\omega t} \\ &= \frac{1}{j\omega} p(x,t) \end{aligned} \quad (\text{B.2})$$

This means that a time integrator has the transfer function $H(\omega) = \frac{1}{j\omega}$.

Hence an ideal integrator has an amplitude response of -20 dB/decade and a phase response of -90° , as shown in Fig.B1.

A phase shift of -90° means that a sinewave is delayed $1/4$ of the period.

Equation (B.2) indicates that time integration can be carried out for a single frequency as a multiplication by $\frac{1}{j\omega}$ in the time domain.

Strictly speaking, this procedure is mathematically incorrect, but is often used, giving valid results under certain assumptions. To some extent this procedure will also be used in these notes.

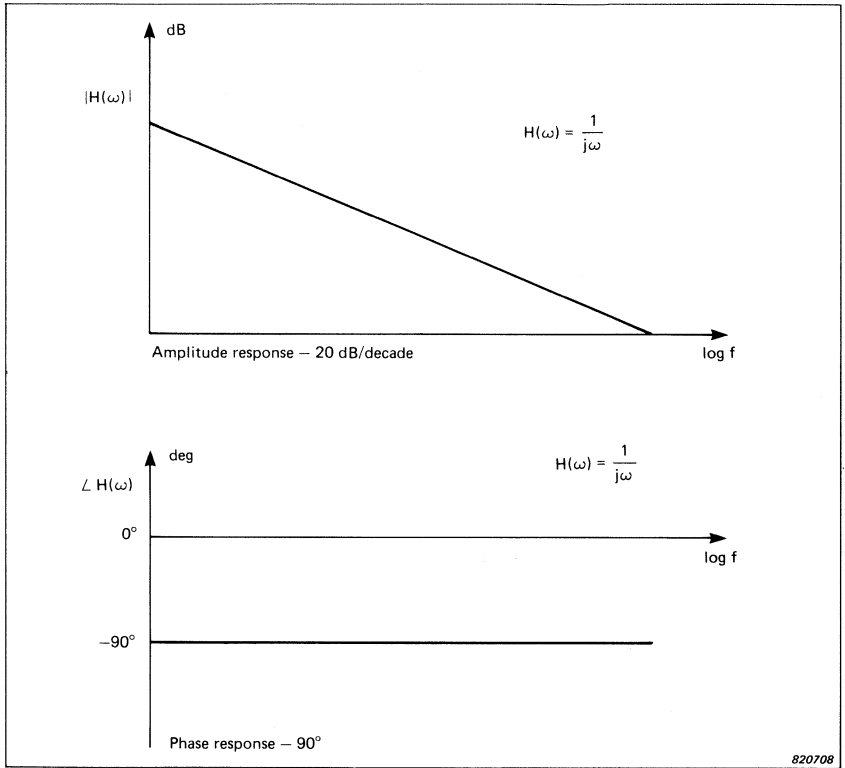


Fig. B1. Amplitude and phase response of an ideal time integrator

APPENDIX C

Active, Reactive Intensity

A phase gradient of the pressure gives a real intensity component, which is caused by a net flow of energy. To show this we need to calculate the reciprocal of the specific impedance, Z_s of the medium, that is the ratio between the particle velocity (the acoustic current) and the pressure (the acoustic voltage).

A modulus gradient gives an imaginary intensity component, which describes the amount of energy that fluctuates between the source and the medium. This means that the reactive intensity is due to a flow of energy in one direction during one part of the cycle, and an exactly equal flow of energy in the opposite direction during the next part of the cycle. The average value of the reactive intensity is of course zero, and makes no contribution to the net flow of energy. It does however, contribute to the total energy density.

If standard complex notation is used and sinusoidal field is assumed, the Equation of motion (equation 3.2) becomes

$$u_r = - \frac{1}{j\omega\rho} \cdot \frac{\partial p}{\partial r} \quad (\text{C.1})$$

Then

$$\begin{aligned} \frac{1}{Z_s} &= \frac{u_r}{p} \\ &= - \frac{1}{j\omega\rho} \frac{\partial p}{\partial r} \cdot \frac{1}{p} \\ &= \frac{j}{\omega\rho} \frac{\partial (\ln p/p_0)}{\partial r} \end{aligned} \quad (\text{C.2})$$

ρ_o is arbitrarily chosen to make the argument of the logarithm function dimensionless.

Inserting $p = |p| \cdot e^{j\phi}$ we obtain

$$\frac{1}{Z_s} = \frac{1}{\rho\omega} \left(-\frac{\partial\phi}{\partial r} + j \frac{\partial(\ln |p|/\rho_o)}{\partial r} \right) \quad (\text{C.3})$$

Equation C.3 shows that

1. If only a phase gradient, $\frac{\partial\phi}{\partial r}$, exists in the sound field (Z_s is real),
then p and u will be in phase.
2. If only a modulus gradient, $\frac{\partial(\ln |p|/\rho_o)}{\partial r}$, exists in the sound field (Z_s is imaginary),
then p and u will be 90° out of phase.

APPENDIX D

FFT Method

For stationary signals we have

$$I(r) = \overline{p(r,t) \cdot u(r,t)} \quad (\text{D.1})$$

where the bar indicates a suitably long averaging time.

$I(r)$ can also be expressed as the cross-correlation function; R_{pu} between $p(r, t)$ and $u(r, t)$. For arbitrary τ we have

$$R_{pu}(r, \tau) = \overline{p(r,t) \cdot u(r, t + \tau)} \quad (\text{D.2})$$

For $\tau = 0$

$$I(r) = R_{pu}(r, 0) \quad (\text{D.3})$$

Now let $S_{pu}(r, f)$ be the cross-spectrum function associated with the cross correlation function $R_{pu}(r, \tau)$. It can be shown that $\text{Re}\{S_{pu}(r, f)\}$ is even and $\text{Im}\{S_{pu}(r, f)\}$ is odd, when $R_{pu}(r, \tau)$ is a real function.

Then by the use of the inverse Fourier Transform we obtain

$$R_{pu}(r, \tau) = \int_{-\infty}^{\infty} S_{pu}(r, f) \cdot e^{j\omega\tau} df$$

and

$$I(r) = R_{pu}(r, 0) = \int_{-\infty}^{\infty} S_{pu}(r, f) \cdot df = \int_{-\infty}^{\infty} \text{Re} \left[S_{pu}(r, f) \cdot df \right] \quad (\text{D.4})$$

which means that the intensity can be calculated from the real part of the cross-spectrum function $S_{pu}(r, f)$.

Let $P(f)$ and $U(f)$ be the Fourier Transforms of $p(t)$ and $u(t)$, respectively, as defined by

$$\begin{aligned} P(f) &= \int_{-\infty}^{\infty} p(t) \cdot e^{-j\omega t} dt \\ U(f) &= \int_{-\infty}^{\infty} u(t) \cdot e^{-j\omega t} dt \end{aligned} \quad (D.5)$$

Then from equation 3.4 and 4.1 it follows

$$\begin{aligned} P(f) &= \frac{1}{2} (P_A(f) + P_B(f)) \\ U(f) &= -\frac{1}{j\omega\rho\Delta r} (P_B(f) - P_A(f)) \end{aligned} \quad (D.6)$$

using the fact that if the Fourier transform of $x(t) dt$ is $X(f)$, then the Fourier transform of $\int x(t) dt$ is $\frac{1}{j\omega} \cdot X(f)$.

By definition (Ref.[12])

$$S_{pu} = E [P^*(f) \cdot U(f)] \quad (D.7)$$

$E[]$ means that ensemble averaging is performed on the quantity inside the brackets. The asterisk $*$ indicates a complex conjugate, which is a change in the sign of the imaginary part, $(x + jy)^* = (x - jy)$. Also note that for the product of two Fourier spectra P and U we have

$$S_{pu}^* = E [(P^* \cdot U)^*] = E [(P \cdot U^*)] = E [(U^* \cdot P)] = S_{up} \quad (D.8)$$

indicating that we just as well could have used

$$S_{up} = E [P(f) \cdot U^*(f)] \quad (D.9)$$

for intensity calculations, since we are only interested in the real part of the cross-spectrum function.

Inserting (D.6) into (D.9) for example gives

$$\begin{aligned} E [P(f) \cdot U^*(f)] &= -\frac{1}{2\omega\rho\Delta r} j E [(P_A(f) + P_B(f)) (P_B^*(f) - P_A^*(f))] \\ &= -\frac{1}{2\omega\rho\Delta r} \left[j (S_{BB} - S_{AA}) - j (S_{AB} - S_{BA}) \right] \end{aligned} \quad (D.10)$$

Now by the use of (D.8) we have

$$\begin{aligned}
 -j (S_{AB} - S_{BA}) &= -j (S_{AB} - S_{AB}^*) \\
 &= -j (j 2 \text{Im } S_{AB}) \\
 &= 2 \text{Im } S_{AB}
 \end{aligned} \tag{D.11}$$

So equation (D.10) can be written as

$$E[P \cdot U^*] = -\frac{1}{2} \frac{1}{\omega \rho \Delta r} \left(j (S_{BB} - S_{AA}) + 2 \text{Im } S_{AB} \right) \tag{D.12}$$

The real part of (D.12), the one sided (only positive frequencies) intensity spectrum is

$$\hat{I}(r, f) = -\frac{2 \text{Im } S_{AB}}{\omega \rho \Delta r} = -\frac{\text{Im } G_{AB}}{\omega \rho \Delta r} \tag{D.13}$$

which is calculated from the imaginary part of the cross-spectrum. S_{AB} denotes 2 sided spectra, while G_{AB} denotes 1 sided spectra.

Finally the desired estimate of the intensity is

$$\hat{I}_r = -\int_0^{\infty} \frac{\text{Im } G_{AB}}{\omega \rho \Delta r} df \tag{D.14}$$

The digital form of equation (D.14) is

$$\hat{I}_r = -\frac{1}{2\pi\rho\Delta r} \sum_{n=1}^{N/2} \frac{\text{Im } G_{AB}(n\Delta f)}{n\Delta f} \tag{D.15}$$

where the summation starts at the lowest frequency $\Delta f = (1/T)$ and stops at the Nyquist frequency $(N/2) \Delta f$.

The imaginary part of (D.12), the one sided reactive intensity spectrum, is

$$\begin{aligned}
 \hat{J}_r(f) &= \frac{1}{\omega \rho \Delta r} (S_{AA} - S_{BB}) \\
 &= \frac{1}{2\omega \rho \Delta r} (G_{AA} - G_{BB})
 \end{aligned} \tag{D.16}$$

which is calculated from the two auto spectra.

APPENDIX E

Approximation Error, Plane Waves

Disregarding the $e^{j\omega t}$ term in equation (B.1.) we obtain:

$$p_A = p_o \cdot e^{-jkr} \quad (\text{E.1})$$

$$p_B = p_o \cdot e^{-jk(r + \Delta r)} = p_A \cdot e^{-jk\Delta r} \quad (\text{E.2})$$

The mean pressure value is (see Fig.E1).

$$p = \frac{1}{2} (p_B + p_A) = \frac{1}{2} p_o (e^{-jk\Delta r} + 1) e^{-jkr} \quad (\text{E.3})$$

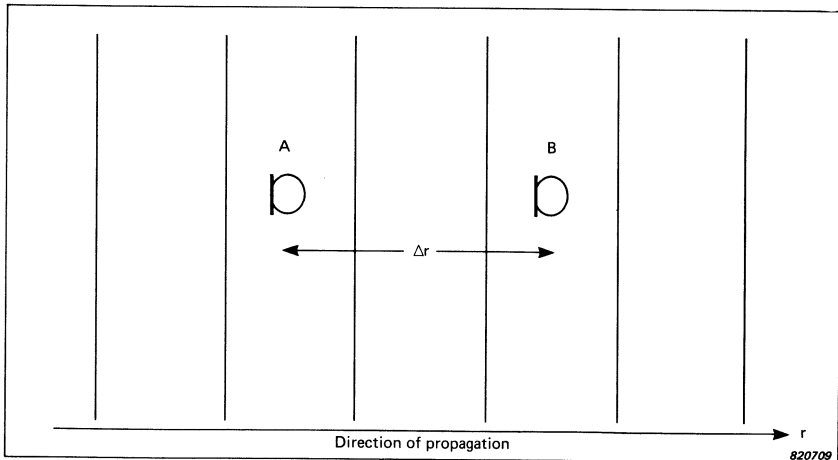


Fig. E1. Probe orientation in a plane progressive wave

The difference between the two pressures is

$$p_B - p_A = p_o \left(e^{-jk\Delta r} - 1 \right) \cdot e^{-jkr} \quad (\text{E.4})$$

Hence the particle velocity will be (using eq. C.1)

$$u_r = - \frac{1}{\rho \Delta r} \frac{1}{j\omega} p_o \left(e^{-jk\Delta r} - 1 \right) e^{-jkr} \quad (\text{E.5})$$

and the complex conjugate of u_r ,

$$u_r^* = \frac{1}{\rho \Delta r} \cdot \frac{1}{j\omega} \cdot p_o \left(e^{jk\Delta r} - 1 \right) e^{jkr} \quad (\text{E.6})$$

We can now calculate the estimated intensity $\hat{I}_r + j \hat{J}_r$, both the real part as well as the imaginary part,

$$\begin{aligned} \hat{I}_r + j \hat{J}_r &= \frac{1}{2} \rho \cdot u_r^* \\ &= \frac{p_o^2}{2\rho c} \frac{1}{k \Delta r} \frac{(e^{-jk\Delta r} + 1)(e^{jk\Delta r} - 1)}{2j} \\ &= \frac{p_{rms}^2}{\rho c} \cdot \frac{1}{k \Delta r} \cdot \frac{(e^{jk\Delta r} - e^{-jk\Delta r})}{2j} \\ &= I_r \cdot \frac{1}{k \Delta r} \cdot \sin(k \Delta r) \\ &= I_r \cdot \frac{\sin(k \Delta r)}{k \Delta r} \end{aligned} \quad (\text{E.7})$$

Notice that $\hat{J}_r = 0$ in this case as expected. A plane, sinusoidal wave is a purely active sound field, i.e. all sound energy is transported, but the

measurement technique underestimates the true value by a $\frac{\sin x}{x}$ function.

If there exists an angle α between the probe orientation and the direction of propagation, the approximation error formula becomes

$$\hat{I}_r = I_r \frac{\sin(k \Delta r \cdot \cos \alpha)}{k \Delta r} \quad (\text{E.8})$$

APPENDIX F

Approximation Error, Spherical Waves

Approximation error from a monopole source. For simplicity the line joining the centres of the microphones passes through the point source. (See Fig.F1).

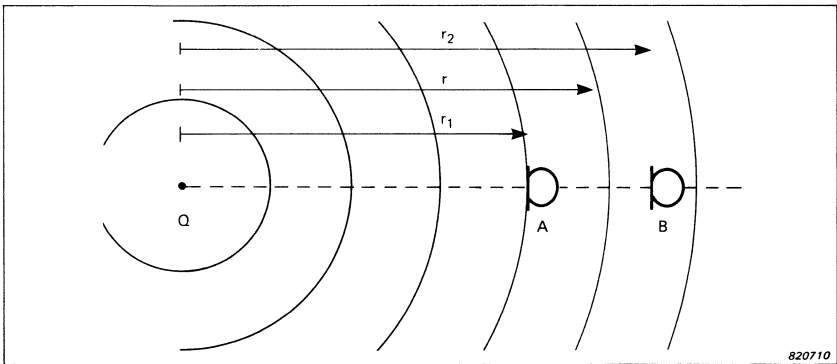


Fig. F1. Probe orientation in a spherical propagating wave

Q is the volume velocity of the source and Φ is the velocity potential.

Thus

$$\Phi = \frac{Q}{4\pi r} \cdot e^{j(\omega t - kr)} \quad (\text{F.1})$$

which gives

$$u_r = -\frac{\partial \Phi}{\partial r} = \left(\frac{1}{r} + jk\right) \left(\frac{Q}{4\pi r}\right) e^{j(\omega t - kr)} \quad (\text{F.2})$$

and

$$p_r = \rho \frac{\partial \Phi}{\partial t} = jk\rho c \cdot \left(\frac{Q}{4\pi r}\right) e^{j(\omega t - kr)} \quad (\text{F.3})$$

Neglecting the term $e^{j\omega t}$ the true intensity at distance r from the source is

$$I_r = \frac{1}{2} \operatorname{Re} (p_r \cdot u_r^*) = \frac{1}{2} \omega k \rho \left(\frac{Q}{4\pi} \right)^2 \frac{1}{r^2} \quad (\text{F.4})$$

By the two microphone technique the measured pressure and velocity will be

$$\begin{aligned} p_m &= \frac{1}{2} (p_B + p_A) \\ &= jk\rho c \frac{1}{2} \left(\frac{Q}{4\pi r_2} e^{-jkr_2} + \frac{Q}{4\pi r_1} e^{-jkr_1} \right) \\ &= -\frac{\omega\rho}{2j} \left(\frac{Q}{4\pi} \right) \left(\frac{e^{-jkr_2}}{r_2} + \frac{e^{-jkr_1}}{r_1} \right) \end{aligned} \quad (\text{F.5})$$

$$\begin{aligned} u_m &= -\frac{1}{j\omega\rho\Delta r} (p_B - p_A) \\ &= -\frac{jk\rho c}{j\omega\rho\Delta r} \left(\frac{Q}{4\pi r_2} e^{-jkr_2} - \frac{Q}{4\pi r_1} e^{-jkr_1} \right) \end{aligned} \quad (\text{F.6})$$

$$u_m^* = -\frac{1}{\Delta r} \left(\frac{Q}{4\pi} \right) \left(\frac{e^{jkr_2}}{r_2} - \frac{e^{jkr_1}}{r_1} \right) \quad (\text{F.7})$$

Hence the estimated intensity is

$$\begin{aligned} \hat{I}_r + j\hat{J}_r &= \frac{1}{2} p_m \cdot u_m^* \\ &= \frac{\omega\rho}{4j\Delta r} \left(\frac{Q}{4\pi} \right)^2 \left(\frac{e^{-jkr_2}}{r_2} + \frac{e^{-jkr_1}}{r_1} \right) \left(\frac{e^{jkr_2}}{r_2} - \frac{e^{jkr_1}}{r_1} \right) \end{aligned} \quad (\text{F.8})$$

We disregard the imaginary part and obtain

$$\begin{aligned}\hat{l}_r &= \frac{\omega\rho}{2\Delta r} \frac{1}{r_1 r_2} \left(\frac{Q}{4\pi}\right)^2 \left(\frac{e^{jk\Delta r} - e^{-jk\Delta r}}{2j}\right) \\ &= \frac{\omega\rho}{2\Delta r} \frac{1}{r_1 r_2} \left(\frac{Q}{4\pi}\right)^2 \sin(k\Delta r)\end{aligned}\quad (\text{F.9})$$

Combining equations (F.4) and (F.9) we obtain

$$\frac{\hat{l}_r}{l_r} = \frac{\sin(k\Delta r)}{k\Delta r} \cdot \frac{r^2}{r_1 r_2} \quad (\text{F.10})$$

Note that

$$\frac{r^2}{r_1 r_2} = \left(1 - \frac{1}{4}\left(\frac{\Delta r}{r}\right)^2\right)^{-1} \quad (\text{F.11})$$

indicating that the near-field influence is a function of the ratio between the microphone separation, Δr and the distance, r between the microphone probe and the acoustic centre of the source.